JOURNAL OF BACTERIOLOGY, Nov. 1990, p. 6386–6395
0021-9193/90/116386-10$02.00/0

Vol. 172, No. 11

Transcription of the Shiga-Like Toxin Type II and Shiga-Like Toxin Type II Variant Operons of *Escherichia coli*

LAWRENCE M. SUNG, MATTHEW P. JACKSON,† ALISON D. O'BRIEN, AND RANDALL K. HOLMES*

Department of Microbiology, The Uniformed Services University of the Health Sciences, 4301 Jones Bridge Road, Bethesda, Maryland 20814-4799

Received 19 April 1990/Accepted 1 September 1990

Shiga-like toxin type II (SLT-II) and Shiga-like toxin type II variant (SLT-IIv) are cytotoxins produced by certain strains of *Escherichia coli*. Nucleotide sequence analyses had revealed that the structural genes for the A subunit and B subunit of SLT-II or SLT-IIv are arranged in an operon. Primer extension and S1 nuclease protection analyses identified a promoter for the *slt*-II operon 118 bases upstream of the *slt*-IIA gene. The *slt*-IIv promoter was demonstrated to be identical to the *slt*-II promoter. The *slt*-II and *slt*-IIv promoters differed significantly from the previously characterized Shiga toxin (*stx*) and Shiga-like toxin type 1 (*slt*-I) promoters. The transcriptional efficiencies of the *stx* and *slt*-II promoters were compared in fusions to the chloramphenicol acetyltransferase gene, and constitutive expression of the *slt*-II promoter was found to be equivalent to derepressed expression of the *stx* promoter. In contrast to the *stx* and *slt*-I promoters, the *slt*-II and *slt*-IIv promoters did not contain sequences for binding of the Fur repressor protein, and SLT-II production was not determined by iron levels in the media in various *E. coli* strains with wild-type or mutant ferric uptake regulation (*fur*) alleles. Northern (RNA) blot analysis demonstrated a single mRNA transcript for the *slt*-II operon, and further analysis of the *slt*-II operon by primer extension did not reveal an independent promoter for the B subunit gene. A putative rho-independent transcription terminator was identified 274 bases downstream of *slt*-IIB. These data indicated that the *slt*-II and *slt*-IIv operons differ from the *stx*/*slt*-I operon in regulation of their transcription by iron. Whether these regulatory differences enable the type I and type II groups of Shiga-like toxins to perform different roles in the pathogenesis of infectious diseases remains to be established.

Enterohemorrhagic *Escherichia coli* strains associated with diarrhea, hemorrhagic colitis, and the hemolytic uremic syndrome in humans and *E. coli* strains responsible for edema disease of swine produce cytotoxins related to Shiga toxin of *Shigella dysenteriae* type 1. These Shiga-like toxins (SLTs; also called verotoxins) include Shiga-like toxin type I (SLT-I), Shiga-like toxin type II (SLT-II), and Shiga-like toxin type II variant (SLT-IIv) and constitute a family whose members are related in structure and biological activities (32). Each toxin is composed of two subunits (9, 34). The A subunit is a single polypeptide with 28S rRNA *N*-glycosidase activity that inhibits protein synthesis (11, 12, 38). The B subunit is oligomeric and mediates binding to specific glycolipid receptors (8, 19, 23–25, 36, 44). The SLTs are cytotoxic for Vero cells, enterotoxic for ligated rabbit ileal segments, and lethal for mice (32). All but SLT-IIv are also cytotoxic for HeLa cells (28).

Shiga toxin and SLT-I are nearly identical proteins referred to as Shiga toxin/SLT-I. Their structural genes, designated *stx* and *slt*-1, differ by only three nucleotides, which translates to a single conservative amino acid difference between the A subunits of the two toxins (41).

The promoters for the *stx* and *slt*-I operons are identical (4, 7, 21, 41), and a Fur-binding site within the promoter sequence permits the iron-dependent regulation of Shiga toxin/SLT-I by the Fur-iron corepressor complex (5). Studies by De Grandis et al. on the *slt*-I operon suggest that *slt*-IA and *slt*-IB are transcribed as a polycistronic mRNA (7). However, their study and previous reports do not preclude the existence of a functional promoter within the downstream sequences of *slt*-IA that could direct the independent transcription of the *slt*-IB gene (7, 30, 46). Evidence for such a second promoter for transcription of *stxB* was reported by Kozlov et al. (22).

The structural genes of SLT-II share 55% nucleotide sequence homology with those of Shiga toxin/SLT-I (20). The sizes of the mature A subunit and B subunit polypeptides of SLT-II, calculated from the deduced amino acid sequences, are 33,135 and 7,817 Da, respectively. The genes coding for the A subunit and B subunit of SLT-II are arranged in tandem with a gap of 14 nucleotides between *slt*-IIA and *slt*-IIB. Putative ribosomal binding sites are located immediately upstream of the A subunit coding region and within the intercistronic gap. The studies reported here were performed to analyze the regulation of transcription of the *slt*-II operon and to compare it with the transcription of the *stx*/*slt*-I operon.

MATERIALS AND METHODS

Bacterial strains and plasmids. *E. coli* HB101 and *E. coli* DH5α were used as hosts for transformation of recombinant plasmids (2) (Bethesda Research Laboratories, Gaithersburg, Md.). *E. coli* JM109 and *E. coli* CJ236 (*dut ung*) were used as hosts for the propagation of bacteriophage M13 (50) (Bio-Rad Laboratories, Richmond, Calif.). *E. coli* AB2847, H1618, and H1646 were kindly provided by Klaus Hantke, Mikrobiologie II, Universität Tübingen, Tübingen, Federal Republic of Germany, and have been described elsewhere (17). The SLT-I converting phage H19J and the SLT-II converting phage 933W have also been described previously

* Corresponding author.
† Present address: Department of Immunology & Microbiology, Wayne State University School of Medicine, Detroit, MI 48201.

TABLE 1. Recombinant plasmids used in this study

Plasmid	Toxin	Description	Reference
pNAS13	Shiga	pBR329 with entire *stx* operon	41
pNN103	SLT-II	pBR328 with entire *slt*-II operon	31
pMJ100	SLT-II	pBS with entire *slt*-II operon	47
pMJ330	SLT-II	pMJ100 with created *Hpa*I site between *slt*-IIA and *slt*-IIB	47
pDLW5	SLT-IIv	pBR329 with entire *slt*-IIv operon	48
pDLW5.125	SLT-IIv	pDLW5 with created *Eco*RI site downsteam of promoter	48
pLMS0.0	Shiga	pNAS13 with created *Bam*HI site downstream of promoter	This study
pLMS1.0	SLT-II	pNN103 with created *Hpa*I and *Bam*HI sites bracketing promoter	This study
pLMS2.1	SLT-II	pLMS1.0 subclone (into pBS) deleting *slt*-II promoter	This study
pLMS2.2	SLT-II	pLMS1.0 subclone (into pBS) retaining *slt*-II promoter	This study
pLMS2.3	SLT-IIv	pDLW5.125 subclone (into pBS) deleting *slt*-IIv promoter	This study
pLMS4.0	NA[a]	pBS with *cat* gene cassette of pCM4	This study
pLMS4.4	NA	pLMS4.4 with *slt*-II terminator between *lac* promoter and *cat*	This study
pLMSCATI	NA	pKK232-8 with *stx* promoter/*cat* transcriptional fusion	This study
pLMSCATII	NA	pKK232-8 with *slt*-II promoter/*cat* transcriptional fusion	This study
pLMSCATC	NA	pKK232-8 with *lac* promoter/*cat* transcriptional fusion	This study

[a] NA, Not applicable.

(33, 40, 42). The recombinant plasmids used in this study are listed in Table 1. Studies using strains transformed with pNAS13 were performed under BL3+EK1 containment conditions prescribed by the guidelines of the National Institutes of Health Recombinant DNA Advisory Committee (13). The following plasmids were used as vectors for cloning and as templates for sequencing and oligonucleotide-directed, site-specific mutagenesis: pBR329 (Boehringer Mannheim Biochemicals, Indianapolis, Ind.), pBS and pBluescript KS (Stratagene, La Jolla, Calif.), and the M13mp18 and M13mp19 replicative form vectors (New England BioLabs, Inc., Beverly, Mass.). The following additional plasmids were used for promoter and transcription terminator analyses: pKK232-8 and pCM4 (Pharmacia LKB Biotechnology, Piscataway, N.J.).

Media, enzymes, biochemicals, and radionuclides. Luria broth (26) or Luria agar was used for routine culturing of bacteria. For iron regulation studies, Chelex (Bio-Rad Laboratories)-treated glucose syncase was used with or without the addition of 10 μg of Fe^{3+} per ml in the form of $FeCl_3$. When required, media were supplemented with antibiotics (Sigma Chemical Co., St. Louis, Mo.) at the following concentrations (μg/ml): ampicillin, 100; streptomycin, 50; chloramphenicol, 50; and tetracycline, 12.5. Agarose for DNA and RNA electrophoresis was purchased from International Biotechnologies, Inc. (New Haven, Conn.).

Restriction enzymes, DNA polymerase I (Klenow fragment), T4 DNA ligase, calf intestinal phosphatase, RNase A, Moloney murine leukemia virus reverse transcriptase, and S1 nuclease were purchased from Boehringer Mannheim Biochemicals. The RNase inhibitor, RNasin, was purchased from Promega Corp. (Madison, Wis.). Lysozyme was purchased from Sigma Chemical Co. Nick translation kits were purchased from Bethesda Research Laboratories, Inc. Sequenase DNA sequencing kits were purchased from U.S. Biochemicals Corp. (Cleveland, Ohio). A nonradioactive chloramphenicol acetyltransferase (CAT) enzyme assay kit was purchased from 5 Prime to 3 Prime, Inc. (West Chester, Pa.). Muta-Gene DNA mutagenesis kits were purchased from Bio-Rad Laboratories. Radionuclides were purchased from Dupont, NEN Research Products (Boston, Mass.).

Preparation of plasmid DNA. Rapid isolations and large-scale preparations of plasmid DNA were done by methods outlined by Maniatis et al. (26). When appropriate, individual restriction fragments were isolated by electroelution by following the instructions supplied by the manufacturer of the electroelution apparatus model UEA 2220 (International Biotechnologies, Inc.).

Transformation. Bacteria were transformed with ligation mixtures or purified plasmid DNA by using the $CaCl_2$ methods described by Hanahan (16) or by the use of an electroporation apparatus (Gene Pulser model 165-2098) by following the methods described by the manufacturer (Bio-Rad Laboratories).

Oligonucleotide synthesis and nucleotide sequence analysis. Synthetic oligonucleotides were prepared with a model 380A DNA synthesizer (Applied Biosystems, Inc., Foster City, Calif.) (Table 2). Nucleotide sequence analysis was done by the dideoxy chain termination method (37) by following the procedure provided by the supplier of the Sequenase DNA sequencing kit (U.S. Biochemicals Corp.).

Cytotoxicity and iron effect assays. Microcytotoxicity assays were done on HeLa and Vero cells according to published modifications (27) of the methods of Gentry and Dalrymple (14). The last dilution of the sample in which greater than or equal to 50% of the HeLa or Vero cells detached from the plastic as assessed by A_{620} measurements was considered the 50% cytotoxic dose (CD_{50}). Tests for regulation of cytotoxin production by iron were performed as described by Weinstein et al. (46). Assays were performed with cultures grown for 24 h at 37°C in Chelex-treated glucose syncase medium with or without the addition of 10 μg of Fe^{3+} per ml as $FeCl_3$.

Isolation of total cellular RNA. Total cellular RNA was isolated by a modification of the guanidinium isothiocyanate RNA extraction procedure (6). Bacterial cultures (40 ml) were grown to mid-logarithmic phase and harvested by centrifugation, and the bacterial pellet was resuspended in 10 ml of a solution containing 15 mM Tris (pH 8.0), 0.45 M sucrose, and 8 mM EDTA. The pellet was then mixed with a solution containing 80 μl of 50 mg/ml lysozyme, 100 μl of 100 mM dithiothreitol, and 10,000 U of RNasin. This suspension was incubated on ice for 15 min and then subjected to centrifugation. Cells were resuspended in 3.5 ml of a solution containing 4 M guanidinium isothiocyanate, 20 mM sodium acetate (pH 5.2), 0.1 mM dithiothreitol, and 0.5% *N*-lauryl sarcosine. The solution was heated for 30 min at 65°C and then drawn through a 20-gauge needle several times. The cell lysate was layered onto 7 ml of 5.7 M cesium chloride and subjected to centrifugation at 30,000 rpm in a

TABLE 2. Oligonucleotides used in this study

Oligonucleotide designation and sequence[a]	Structural gene and oligonucleotide position[b]	Purpose
Primer extensions		
PEII1 5'-AAACCCAGTAACAGGCACAGTACC-3'	*slt*-IIA, +47 to +24	*slt*-II promoter search
PEII3 5'-ATAATATACACTTCATATACAGGTG-3'	*slt*-IIA, +16 to −9	*slt*-II promoter search
PEIIV4 5'-GTAATCAGTACCAGACCCGGCGCA-3'	*slt*-IIvA, +48 to +25	*slt*-IIv promoter search
PEIIB5 5'-CGCCATTGCATTAACAGAAGC-3'	*slt*-IIB, +57 to +37	Independent *slt*-IIB promoter search
PEIIB6 5'-TGTCATCCTCATTATACTTGG-3'	*slt*-IIB, +109 to +89	Independent *slt*-IIB promoter search
Site-specific mutagenesis		
RECHP1 5'-CGGCTGAGTTAACAACGCATAATGC-3'	*slt*-IIA, −150 to −174	Creation of *Hpa*I site in *slt*-II
RECBH1 5'-TGTACTGGATCCGAACCAGTGACCG-3'	*slt*-IIA, −99 to −123	Creation of *Bam*HI site in *slt*-II
STXBH1 5'-AATACTCCTTGGGATCCATACGAT-3'	*stxA*, −12 to −34	Creation of *Bam*HI site in *stx*
Sequencing primers		
S1II2 5'-GGGAATAGGATACCGAAGAAAAACCC-3'	*slt*-IIA, +67 to +42	S1 nuclease sequence ladder
SLTII9 5'-GTGGGGCGACTGGTG-3'	*slt*-IIB, +124 to +139	Sequence data (*slt*-II terminator)

[a] The oligonucleotides (with the exception of SLTII9) correspond to the nonmessage-sense strand. SLTII9 corresponds to the message-sense strand.
[b] The positions of the oligonucleotides (with the exception of SLTII9) are listed relative to the initiation codon (+1 adenine) of the respective toxin structural gene. SLTII9 is located 124 to 139 nucleotides downstream of the stop codon of *slt*-IIB.

Beckman SW40.1 rotor at 20°C for 12 h. The RNA pellet was resuspended in water and dispensed into aliquots, and each aliquot was precipitated with ethanol.

Primer extension analysis. Total cellular RNA (50 μg) and 25 ng of a ^{32}P-5'-end-labeled oligonucleotide primer was coprecipitated and resuspended in 30 μl of a solution containing 40 mM PIPES [piperazine-*N*,*N*'-bis(2-ethanesulfonic acid); pH 6.7], 1 mM EDTA, 0.2% sodium dodecyl sulfate, and 0.4 M sodium chloride. The mixture was heated to 80°C for 5 min and then at 37°C for 2 h to permit the annealing of the oligonucleotide primer to the RNA. This RNA-primer complex was then precipitated with ethanol, and the precipitate was resuspended in 50 μl of the following solution: 50 mM Tris hydrochloride (pH 8.3), 6 mM magnesium chloride, 40 mM potassium chloride, 10 mM dithiothreitol, 2.5 μl each of 10 mM dNTP (dATP, dGTP, dCTP, and dTTP), and 20 U of Moloney murine leukemia virus reverse transcriptase. Extension of the oligonucleotide primer to the 5' terminus of the RNA was allowed to proceed for 2 h. The RNA-DNA complex was then treated with 1 μl of a 10 mg/ml RNase A solution, extracted with phenol-chloroform, and precipitated with ethanol. The pellet was resuspended in 5 μl of formamide loading buffer and subjected to polyacrylamide gel electrophoresis on a vertical sequencing gel apparatus. Dideoxy chain termination sequencing reaction mixtures were used as nucleotide length markers.

To map the promoter upstream of *slt*-IIA, the nonmessage-sense sequence ladder was generated by using the message-sense strand of the 1,100-bp *Sph*I-*Eco*RV fragment of pNN103 (Table 1) in M13mp19 as the template and either oligonucleotide PEII1 or PEII3 (Table 2) as the primer. To map the promoter upstream of *slt*-IIvA, the nonmessage-sense sequence ladder was generated by using the message-sense strand of the 4,200-bp *Aat*II-*Cla*I fragment of pDLW5 (Table 1) in M13mp19 as the template and oligonucleotide PEIIV4 (Table 2) as the primer. To attempt to locate an independent *slt*-IIB promoter, the nonmessage-sense sequence ladder was generated with the message-sense strand of the 772-bp *Eco*RV-*Pst*I fragment of pNN103 (Table 1) in M13mp19 as the template and either oligonucleotide PEIIB5 or PEIIB6 (Table 2) as the primer.

S1 nuclease protection analysis. Total cellular RNA (50 μg) from *E. coli* HB101(pNN103) and 50 ng of a ^{32}P-5'-end-labeled 1,030-bp *Sph*I-*Sma*I fragment of pNN103 (Table 1) were coprecipitated and resuspended in 20 μl of a solution containing 40 mM PIPES (pH 6.8), 90% formamide, 0.4 M sodium chloride, and 1 mM EDTA. The mixture was heated at 90°C for 10 min, and the RNA and DNA fragments were permitted to anneal at 49°C for 12 h. The RNA-DNA complex was then analyzed as described above for primer extension analysis. The reference ladder represents the nonmessage-sense strand sequence and was generated by using the message-sense strand of the 1,100-bp *Sph*I-*Eco*RV fragment of pNN103 (Table 1) in M13mp19 as the template and the oligonucleotide S1II2 (Table 2) as the primer.

Confirmation of the *slt*-II operon terminator. The nucleotide sequence of regions downstream of the *slt*-IIB open reading frame was examined by computer homology search with the Genetics Computer Group (University of Wisconsin, Madison, Wis.) sequence analysis package. The computer program, Terminator, was used to search for putative procaryotic factor-independent RNA polymerase terminators according to the algorithm of Brendel and Trifonov (3). The 50-bp *Stu*I-*Nru*I fragment of pNN103, which contained the *slt*-II transcription terminator, was inserted into pLMS4.0 (Table 1) between the *lac* promoter and the translation start codon of the chloramphenicol acetyltransferase gene (*cat*) to create pLMS4.4 (Table 1). The activity of this construct was determined by CAT enzyme-linked immunosorbent assay.

Northern (RNA) blot analysis. Total cellular RNA (50 μg) from *E. coli* HB101(pNN103) was dissolved in a solution containing 22.5 μl of dimethyl sulfoxide, 4.5 μl of sodium phosphate (pH 7), and 6.6 μl of glyoxal. This solution was incubated at 37°C for 1 h and was cooled on ice, and 12 μl of glyoxal loading buffer was added. The samples were subjected to electrophoresis in a 1.2% agarose gel at 4 V/cm with constant buffer recirculation. rRNAs (23S, 16S, and 5S) were run alongside the samples as size standards. The RNA was transferred onto nitrocellulose by using a Vacu-Blot apparatus (Pharmacia LKB Systems). The nitrocellulose filter was baked at 80°C for 2 h in a vacuum oven and soaked in a prehybridization solution (39) for at least 2 h. Filters were probed with either a ^{32}P-labeled 460-bp *Hpa*I-*Kpn*I fragment of pMJ330 (Table 1) which contains only *slt*-IIB subunit coding sequences or a ^{32}P-labeled 1,350-bp *Sma*I-*Kpn*I fragment of pMJ330 which contains both *slt*-IIA and *slt*-IIB coding sequences.

Oligonucleotide-mediated, site-directed mutagenesis. To create restriction sites in the SLT-II operon, a M13mp19 vector containing the 1,100-bp *Sph*I-*Eco*RV fragment of pNN103 (Table 1) was propagated in *E. coli* CJ236. The single-stranded DNA template was annealed to RECHP1 (Table 2), an oligonucleotide designed to create an *Hpa*I site 162 nucleotides upstream of *slt*-IIA. The resulting single-stranded template which contained the *Hpa*I site was propagated in *E. coli* CJ236 as described above and subsequently used with the mutagenic oligonucleotide RECBH1 (Table 2) to introduce a *Bam*HI site 110 nucleotides upstream of *slt*-IIA. A 1,030-bp *Sph*I-*Sma*I fragment containing both newly introduced sites was ligated with the 2,200-bp *Sma*I-*Eco*RI fragment of pNN103 into vector pBR329 to construct pLMS1.0 (Table 1).

To create a restriction site between the promoter and structural genes in the Shiga toxin operon, an M13mp19 vector containing the 725-bp *Bgl*II-*Hin*dIII fragment of pNAS13 (Table 1) was propagated in *E. coli* CJ236. The single-stranded DNA template was annealed to STXBH1 (Table 2), an oligonucleotide designed to create a *Bam*HI site 24 nucleotides upstream of *stxA*. A 746-bp *Eco*RI-*Hin*dIII fragment containing the newly introduced site was ligated to the 1,800-bp *Hin*dIII-*Eco*RI fragment of pNAS13 into vector pBR329 to construct pLMS0.0 (Table 1).

Creation of promoter-deletion constructs. Shiga-like toxin promoter-deletion subclones were constructed (see Fig. 6). The 2,445-bp *Hpa*I-*Eco*RI fragment of pLMS1.0 was cloned into vector pBluescript KS to construct pLMS2.1 (Table 1). The 2,395-bp *Bam*HI-*Eco*RI fragment of pLMS1.0 was cloned into vector pBluescript KS to construct pLMS2.2 (Table 1). The 3,800-bp *Eco*RI-*Cla*I fragment of pDLW5.125 was cloned into vector pBluescript KS to construct pLMS2.3 (Table 1). Each fragment was inserted into pBluescript KS in an orientation opposite to the direction of transcription from the promoters for the *lacZ* and ampicillin resistance genes.

Creation of Shiga-like toxin promoter/CAT transcriptional fusions. The 139-bp *Bgl*II-*Bam*HI fragment of pLMS0.0, which contains the *stx* promoter, was cloned into the promoter analysis vector pKK232-8 to create pLMSCATI (Table 1). The 51-bp *Hpa*I-*Bam*HI fragment of pLMS1.0, which contains the *slt*-II promoter, was cloned into pKK232-8 to create pLMSCATII (Table 1). The 216-bp *Pvu*II-*Hin*dIII fragment of pBS, which contains the *lac* promoter, was cloned into pKK232-8 to create pLMSCATC (Table 1). The activities of these constructs in *E. coli* DH5α were determined by CAT enzyme-linked immunosorbent assay.

RESULTS AND DISCUSSION

Promoter mapping of the SLT-II and SLT-IIv operons. To identify the transcription start site for the SLT-II operon, primer extension experiments were performed with oligonucleotide primer PEIII (Table 2) using total cellular RNA isolated from either the SLT-II clone *E. coli* HB101 (pNN103) (Fig. 1) or the SLT-II phage lysogen *E. coli* C600 (933W) (data not shown). In both cases, a band was observed that comigrated with chains terminated at a specific thymine in the sequence ladder. This band represented an extension of 142 bases to a position located 118 nucleotides upstream of the *slt*-IIA initiation codon and corresponded to an adenine residue in the message-sense strand. No bands were observed with control primer extension reactions using total cellular RNA from an *E. coli* HB101 strain.

The location of the *slt*-II transcription start site was

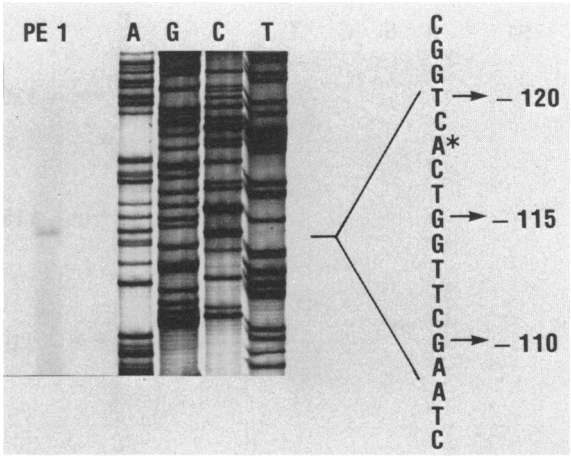

FIG. 1. Primer extension analysis. Total cellular RNA isolated from *E. coli* HB101(pNN103) was probed with oligonucleotide primer PEII1 (Table 2). The dideoxy sequence ladder represents the nonmessage-sense strand sequence and was generated with the message-sense strand of the 1,100-bp *Sph*I-*Eco*RV fragment of pNN103 (Table 1) in M13mp19 as the template and oligonucleotide PEII1 as the primer. The sequence of the corresponding message-sense strand is shown at the right, with the 5′ end at the top and the 3′ end at the bottom. A band was observed to comigrate with chains terminated at a thymine, which corresponds to an adenine residue (*) on the message-sense strand located 118 nucleotides upstream of the *slt*-IIA initiation codon.

independently established by using a second oligonucleotide primer, PEII3 (Table 2), in additional primer extension experiments with total cellular RNA from *E. coli* HB101 (pNN103) (Fig. 2). A transcript of 109 bases was observed, which reflects an extension to the same nucleotide position upstream of *slt*-IIA that was previously identified. There-

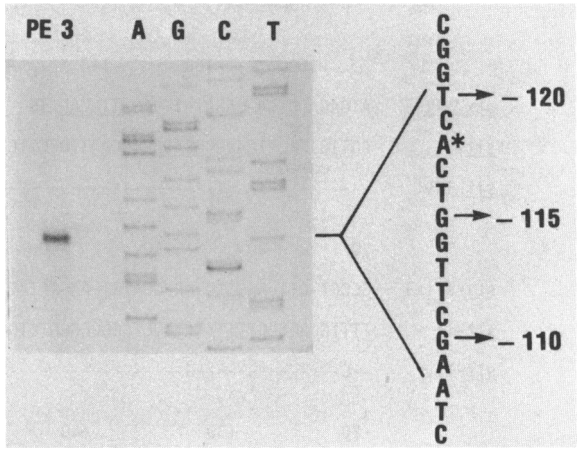

FIG. 2. Primer extension analysis. Total cellular RNA isolated from *E. coli* HB101(pNN103) was probed with oligonucleotide primer PEII3 (Table 2). The dideoxy sequence ladder represents the nonmessage-sense strand sequence and was generated with the message-sense strand of the 1,100-bp *Sph*I-*Eco*RV fragment of pNN103 (Table 1) in M13mp19 as the template and oligonucleotide PEII3 as the primer. The sequence of the corresponding message-sense strand is shown at the right, with the 5′ end at the top and the 3′ end at the bottom. A band was observed to comigrate with chains terminated at a thymine, which corresponds to an adenine residue (*) on the message-sense strand located 118 nucleotides upstream of the *slt*-IIA initiation codon.

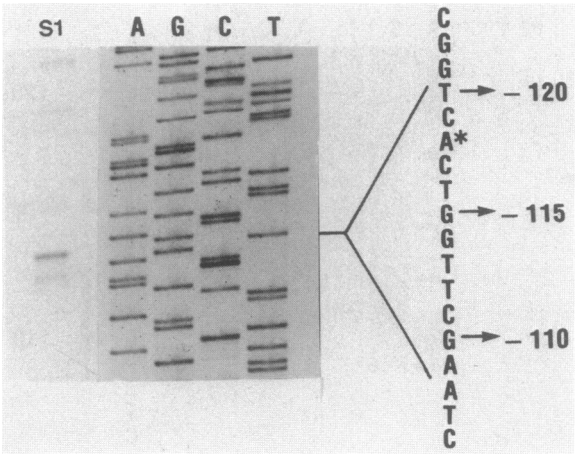

FIG. 3. S1 nuclease protection analysis. Total cellular RNA isolated from *E. coli* HB101(pNN103) was probed with the 1,030-bp *Sph*I-*Sma*I fragment of pNN103 (Table 1), which includes the first 67 nucleotides of *slt*-IIA and sequences upstream. The dideoxy sequence ladder represents the nonmessage-sense strand sequence and was generated with the message-sense strand of the 1,100-bp *Sph*I-*Eco*RV fragment of pNN103 in M13mp19 as the template and oligonucleotide S1II2 as the primer (Table 2). The sequence of the corresponding message-sense strand is shown at the right, with the 5′ end at the top and the 3′ end at the bottom. A band comigrated with chains terminated at a thymine, which corresponds to an adenine residue (*) on the message-sense strand located 118 nucleotides upstream of the *slt*-IIA initiation codon.

fore, primer extensions from two independent positions within the *slt*-IIA gene identified the adenine residue 118 nucleotides upstream of the *slt*-IIA open reading frame on the message-sense strand as the transcription start site.

Primer extension analysis was also used to search for a possible second promoter for the transcription of the B subunit. Two oligonucleotides, PEIIB5 and PEIIB6 (Table 2), designed to anneal at different positions within *slt*-IIB were used. No transcription start sites could be identified in these primer extension experiments. These experiments provide no evidence for a second promoter for independent transcription of the *slt*-IIB gene.

As a second method of identifying the transcription start site for the SLT-II operon, RNA transcripts from *E. coli* HB101(pNN103) were examined by S1 nuclease protection studies. A 185-bp fragment protected from S1 nuclease digestion comigrated with chains terminated at a thymine in the sequence ladder (Fig. 3), which again corresponds to the adenine residue 118 nucleotides upstream of the *slt*-IIA open reading frame on the message-sense strand.

Because of the high degree of nucleotide sequence homology between *slt*-II and *slt*-IIv (15, 20, 48), primer extension analysis was performed to identify the *slt*-IIv promoter and compare it with the putative *slt*-II promoter. Using total cellular RNA isolated from the SLT-IIv clone, *E. coli* HB101 (pDLW5), and the oligonucleotide PEIIV4 (Table 2), a transcription start site was identified at an adenine residue 119 nucleotides upstream of the *slt*-IIvA initiation codon (data not shown). Alignment of the nucleotide sequences upstream of *slt*-IIA and *slt*-IIvA revealed the addition of a single base at position −91 of *slt*-IIv (Fig. 4). Therefore, the −119 adenine of *slt*-IIv is homologous to the −118 adenine of *slt*-II. A further sequence comparison indicated that *slt*-II and *slt*-IIv differ by only two nucleotides in this region (Fig. 4). On the basis of the transcription start sites identified, the −35 and −10 promoter sequences for *slt*-II and *slt*-IIv are identical.

The −35 and −10 sequences of the *slt*-II/*slt*-IIv promoter are not homologous to those of the *stx*/*slt*-I promoter (4, 5, 7, 22), nor do they conform well to the consensus −35 and −10 sequences established from a compilation of known *E. coli* promoters (18, 35). No Fur repressor-binding site was found in the *slt*-II/*slt*-IIv promoter region (15, 20, 48), in contrast to sequences reported for the *stx*/*slt*-I promoter (4, 5, 7, 21, 22, 41).

```
                -160      -150      -140      -130      -120      -110      -100       -90       -80
stx/slt-I   ATGAGA-CTGA-CAGAT-TT-AG-TTGCAG-TC---TT-A-TAT-A-TATCAT--TC-T-A-GT--TTGTTACGTT---CCGG-GCG-C-TAAAA-
slt-II      CGTTGTTAGCTCAGCCGGACAGAGCAATTGCCTTCTGAGCAATCGGTCACTGGTTCGAATCCAGTACAACGCGCCATATTTATTTACCAGGCTCGC
slt-IIv     -------------T--------------------A-----------------------------------+AC--AT---C--T-------

           -70       -60       -50       -40       -30       -20       -10        +1         +10
stx/slt-I   GCCGT-CTT-AGGGCG-GG-GGATGT-AA-AATATAGTTATCG--TGGTGCT---GGA-T-TTGTGTA-- ATG --A ATA --T A-T ---
slt-II      TTTTGCGGGCCTTTTTTATATCTGCGCCGGGTCTGGTGCTGATTACTTCAGCCAAAAGGAACACCTGTAT ATG AAG TGT ATA TTA TTT
slt-IIv     --C-------------G-----------------A-----------A-T--------T-TA----- ATG --- --- --- --G --A

            +20         +30         +40         +50         +60         +70
stx/slt-I   -G- GT- C-- ACT -TT T-C --T G-T ATC --- --A GTT AAT GTG GTG G-G AA- --A
slt-II      AAA TGG GTA CTG TGC CTG TTA CTG GGT TTT TCT TCG GTA TCC TAT TCC CGG GAG
slt-IIv     --G --- A-- --- --T --- --- --- --- --- --- --- --- --- --- --- -A- ---
```

FIG. 4. Previously determined nucleotide sequences for *stx*/*slt*-I, *slt*-II, and *slt*-IIv aligned with respect to the initiation codon for the A subunit. A dash (-) represents a nucleotide identical at the position as compared with *slt*-II. A single-base addition (+) occurs at position −91 of *slt*-IIv. Underlined are the −35 and −10 promoter sequences for the respective operons, the −118 adenine transcription start site for the SLT-II operon, and the −60 novel transcription start site identified in the promoter-deletion subclone pLMS2.2. The Fur protein-binding sequence, as determined by Calderwood et al. (4), extends from −129 to −108 on the *stx*/*slt*-I nucleotide sequence. In addition, the locations of restriction endonuclease sites created by oligonucleotide-directed, site-specific mutagenesis are indicated. Symbols: ○, *Bgl*II site in *stx*; ⊖, *Hpa*I site in *slt*-II; ⊙, *Bam*HI site in *slt*-II; ⊗, *Eco*RI site in *slt*-IIv; and ⊕, *Bam*HI site in *stx*.

TABLE 3. Effects of iron on SLT-II production

E. coli lysogen[a]	Toxin	*fur* gene[b]	Iron[c]	Cytotoxin (mean ± 2 SEM)[d]		
				Cell-associated	Extracellular	Total/A_{600}
AB2847(H19J)	SLT-I	+	+	7.5 ± 0.2[e]	8.6 ± 0.3	7.5 ± 0.4[e]
			−	8.6 ± 0.2	8.6 ± 0.2	8.5 ± 0.3
H1618(H19J)	SLT-I	−	+	6.5 ± 0.3	6.8 ± 0.3	6.9 ± 0.4
			−	6.8 ± 0.2	7.0 ± 0.3	7.1 ± 0.3
H1646(H19J)	SLT-I	+++	+	7.0 ± 0.3[e]	6.5 ± 0.3	6.6 ± 0.3[e]
			−	8.4 ± 0.1	6.8 ± 0.2	8.1 ± 0.2
AB2847(933W)	SLT-II	+	+	5.4 ± 0.2	6.5 ± 0.7	5.9 ± 0.5
			−	5.2 ± 0.1	6.5 ± 0.6	5.9 ± 0.4
H1618(933W)	SLT-II	−	+	3.1 ± 0.1	3.6 ± 0.2	3.6 ± 0.2
			−	3.1 ± 0.1	3.9 ± 0.3	3.7 ± 0.3
H1646(933W)	SLT-II	+++	+	3.2 ± 0.2	3.1 ± 0.3	3.0 ± 0.2
			−	3.1 ± 0.1	3.2 ± 0.1	3.0 ± 0.1

[a] Four samples tested per group.
[b] +, Single chromosomal *fur* copy; +++, multiple plasmid *fur* copies; −, point mutation in chromosomal *fur* copy, Fur null phenotype.
[c] +, With added iron; −, without added iron.
[d] Cell-associated, $\log_{10}$ CD_{50} per pellet; Extracellular, $\log_{10}$ CD_{50} per 50 ml of supernatant; Total/A_{600}, $\log_{10}$ cell-associated CD_{50} plus $\log_{10}$ extracellular CD_{50} divided by A_{600}. Results are expressed as mean values ± 2 standard errors of the mean.
[e] Significantly different ($P < 0.05$) by Student's unpaired *t* test from value for the same lysogen grown in the absence of added iron.

Iron regulation of SLT-II. Shiga toxin/SLT-I production has been shown by several groups to be repressed by high levels of iron, whereas SLT-II and SLT-IIv production are not influenced by the concentration of iron in the media (10, 29, 43, 46, 48). Iron regulation of the SLT-I operon is mediated by the binding of the Fur protein and its iron corepressor to a site within the *slt*-I promoter which prevents transcription of the toxin genes (5).

We compared the expression of prophage-encoded *slt*-I and *slt*-II genes in several *E. coli* strains that differ with respect to the presence or absence of the *fur* allele and its copy number (Table 3). The SLT-I-converting phage H19J or the SLT-II-converting phage 933W was lysogenized into three different *E. coli* strains: AB2847, which contains the chromosomal *fur*$^+$ allele; H1618, a *fur* mutant of AB2847; and H1646, constructed by introducing the high-copy-number *fur* plasmid pMH1 into strain H1618. In each of these strains, the expression of the prophage-encoded *slt*-I or *slt*-II operon was compared under low-iron and high-iron growth conditions. SLT-I production was iron regulated in the H19J *fur*$^+$ lysogens AB2847(H19J) and H1646(H19J) but not in the H19J *fur* lysogen H1618(H19J), confirming previous reports. Under identical conditions, SLT-II production, as seen in 933W lysogens AB2847(933W), H1618(933W), and H1646 (933W), was independent of the iron concentration and the copy number of the *fur* gene. These findings confirm and extend the conclusion that the *fur* gene product plays no role in the regulation of the SLT-II operon. It is noteworthy that SLT-II levels were several hundredfold greater in the AB2847 lysogens than in H1618 of H1646 lysogens. The genetic basis for this difference between the host strains of bacteria was not determined.

Terminator mapping of the SLT-II operon. A computer search for sequence homology with a consensus sequence for known *E. coli* terminators revealed a potential rho-independent transcription termination sequence 274 bp downstream of *slt*-IIB. To confirm that the predicted sequence functions as a transcription terminator, the putative terminator sequence was inserted into pLMS4.0 (Table 1) between the *lac* promoter and the chloramphenicol acetyltransferase (*cat*) gene. The resultant construct, pLMS4.4 (Table 1), produced 100-fold less CAT protein than pLMS4.0. This finding demonstrated the functional activity of the proposed *slt*-II terminator. Rho independence of the terminator was not tested.

Transcriptional analyses of the SLT-II operon. Previous reports on the mechanism of transcription of the SLT-I operon provided some evidence that a second promoter might exist within the downstream sequences of the *slt*-IA open reading frame (7, 30, 46). Furthermore, an examination of the transcription of the Shiga toxin operon by Northern blot analysis revealed both a polycistronic message and a putative B subunit message (22). An independent transcriptional start site for *stx*/*slt*-IB could lead to increased expression of the B subunit gene and help explain the single A subunit to multiple B subunit protein stoichiometry observed in the holotoxin.

Transcripts of the SLT-II operon were examined by Northern blot analysis. Filters were probed with a DNA fragment containing both *slt*-IIA and *slt*-IIB sequences. A single band was observed (Fig. 5A) which corresponded to the expected size of a transcript proceeding from the putative *slt*-II promoter to the terminator. When the same blots were probed with a smaller DNA probe containing only *slt*-IIB sequences, the same band was observed (Fig. 5B). With neither probe were other bands apparent, even after prolonged exposure of the autoradiographs. The results reported here of Northern blot and primer extension analyses of *slt*-II clearly indicated that transcription of the SLT-II operon occurs as a single unit and provide no evidence for an independent promoter for the *slt*-IIB gene.

The regulation of protein subunit synthesis in the SLT-II operon may be analogous to that for the cholera toxin (*ctx*) operon. Cholera toxin, which exists as a single A subunit with five B subunits, is also translated from a polycistronic message (1). The B subunit open reading frame is translated more efficiently than the A subunit open reading frame from the cholera toxin polycistronic mRNA. Two mechanisms have been proposed to account for this difference. The ribosome-binding site contiguous to *ctxB* functions more efficiently than the ribosome-binding site adjacent to *ctxA*. Differences in secondary structure of the cholera toxin mRNA between the *ctxA* and *ctxB* regions could also result in different rates of synthesis of the A subunit and B subunit polypeptides of cholera toxin (49). Explanations similar to those proposed for the translational control of the cholera

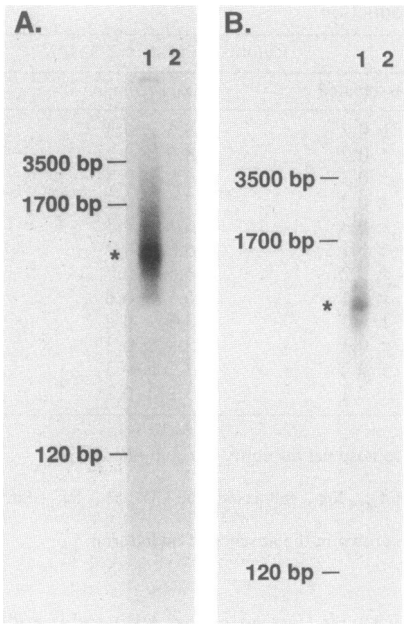

FIG. 5. Northern blot analysis. Total cellular RNA was denatured with glyoxal-dimethyl sulfoxide, subjected to electrophoresis on a 1.4% agarose gel, and transferred to nitrocellulose. Lanes 1 and 2, Total cellular RNA isolated from *E. coli* HB101(pNN103) and an *E. coli* HB101(pBR329) control, respectively. (A) Filter probed with a 1,350-bp *Sma*I-*Kpn*I fragment of pMJ330 (Table 1) which contains both *slt*-IIA and *slt*-IIB coding sequences. (B) Filter probed with a 460-bp *Hpa*I-*Kpn*I fragment of pMJ330 (Table 1) which contains only *slt*-IIB subunit coding sequences. *, Band corresponding to transcript.

toxin operon may be applicable to the SLT-II operon, but experimental data are not yet available for SLT-II.

Functional analysis of the *slt*-II/*slt*-IIv promoter. Oligonucleotide-directed, site-specific mutagenesis was used to create *Hpa*I and *Bam*HI restriction endonuclease sites bracketing the putative *slt*-II promoter sequences in plasmid pLMS1.0 (Table 1) as well as a *Bam*HI site downstream of the *stx* promoter in plasmid pLMS0.0 (Table 1). These new restriction sites permitted the isolation of the promoter sequences for an examination of transcriptional activity. Promoter-deletion subclones were analyzed to establish that the putative promoter sequences mapped by primer extension and S1 nuclease protection studies were indeed the functional promoters for the SLT-II and SLT-IIV operons.

Sequences adjacent to the *Hpa*I site upstream of the putative *slt*-II promoter were deleted in pLMS2.1 (Fig. 6). *E. coli* DH5α(pLMS2.1) produced 10^3 CD_{50}/ml of SLT-II (Table 4). Next, the *Hpa*I-*Bam*HI fragment containing the putative *slt*-II promoter was also deleted during the construction of pLMS2.2 (Fig. 6). Surprisingly, *E. coli* DH5α (pLMS2.2) was also cytotoxic at 10^3 CD_{50}/ml. Primer extension analysis performed on total RNA isolated from the promoter-deletion subclone pLMS2.2 revealed a new transcription start site 60 nucleotides upstream of the *slt*-IIA open reading frame (Fig. 4). Cytotoxin production by *E. coli* DH5α(pLMS2.2) was therefore attributed to transcription of the SLT-II genes from a secondary promoter, which is inactive in the wild-type SLT-II operon. Direct confirmation that the *Hpa*I-*Bam*HI fragment contains a functional promoter was provided by the operon fusion experiments described in the next section.

TABLE 4. Cytotoxicity of promoter-deletion subclones in *E. coli* DH5α

Plasmid construct[a]	Toxin operon	Promoter[b]	Cytotoxicity[c]
pNN103	SLT-II	+	10^4
pLMS1.0	SLT-II	+	10^4
pLMS2.1	SLT-II	+	10^3
pLMS2.2	SLT-II	−	10^{3d}
pDLW5	SLT-IIv	+	10^3
pDLW5.125	SLT-IIv	+	10^3
pLMS2.3	SLT-IIv	−	BLD[e]

[a] As described in Table 1.
[b] +, Putative promoter present; −, putative promoter deleted.
[c] CD_{50} of sonically disrupted cells.
[d] Production of SLT-II by this strain reflects activity of a secondary promoter that was exposed when the primary promoter was deleted (see text).
[e] BLD, Below the limit of detection, less than 10^1 CD_{50}.

The putative *slt*-IIv promoter located within the *Aat*II-*Eco*RI fragment of pDLW5.125 was deleted in the construction of pLMS2.3 (Fig. 6). No detectable toxin activity (less than 10^1 CD_{50}/ml) was observed with *E. coli* DH5α (pLMS2.3) (Table 4). In contrast, *E. coli* DH5α harboring pDLW5.125 (Fig. 6), which retained the putative *slt*-IIv promoter sequences, was cytotoxic at 10^3 CD_{50}/ml. These data support the assignment of the *slt*-IIv promoter on the basis of nucleotide sequence and primer extension analysis.

Comparison of transcriptional efficiencies of the *stx* and *slt*-II promoters. In contrast to the *stx*/*slt*-I promoter, which was previously mapped by primer extension, the nucleotide sequence of the *slt*-II promoter is not highly homologous to a consensus sequence established from a compilation of defined *E. coli* promoters. Promoters which lack homology with the consensus sequence are generally less efficient at initiating transcription than promoters with a high degree of homology (18, 35). Thus, we initially reasoned that the *slt*-I promoter might be a more-effective transcription start signal than the *slt*-II promoter. In support of this hypothesis was the observation that the cytotoxic activities observed in cell lysates of SLT-I-producing enterohemorrhagic *E. coli* strains are 100- to 1,000-fold higher than for SLT-II- or SLT-IIv-producing strains (32). The transcriptional activities of the *stx* and the *slt*-II promoters were examined by using the promoter analysis vector pKK232-8, in which the expression of the chloramphenicol acetyltransferase (*cat*) gene is regulated by the heterologous promoter fragment inserted. The amounts of CAT enzyme produced by the *fur*$^+$ strain *E. coli* DH5α harboring the *stx* promoter/*cat* fusion pLMSCATI (Table 1) and the *slt*-II promoter/*cat* fusion pLMSCATII (Table 1) were compared at different iron concentrations in the growth media (Table 5). The CAT activity for the *slt*-II promoter/*cat* fusion strain was similar under high- and low-iron conditions and was comparable to that of the *stx* promoter/*cat* fusion strain under low-iron conditions. However, the *stx* promoter fusion produced significantly lower levels of CAT enzyme under high-iron conditions. These data confirm that the *stx* promoter activity is regulated by iron and establish that the constitutive activity of the *slt*-II promoter is comparable with the derepressed activity of the *stx* promoter. Therefore, it is likely that the significant differences observed in the production of SLT-I and SLT-II by toxinogenic clinical isolates of *E. coli* are not directly related to differences in the transcriptional efficiencies of the *stx*/*slt*-I and *slt*-II/*slt*-IIv promoters.

In summary, the promoters for the SLT-II and SLT-IIv operons were identified and found to be identical. The

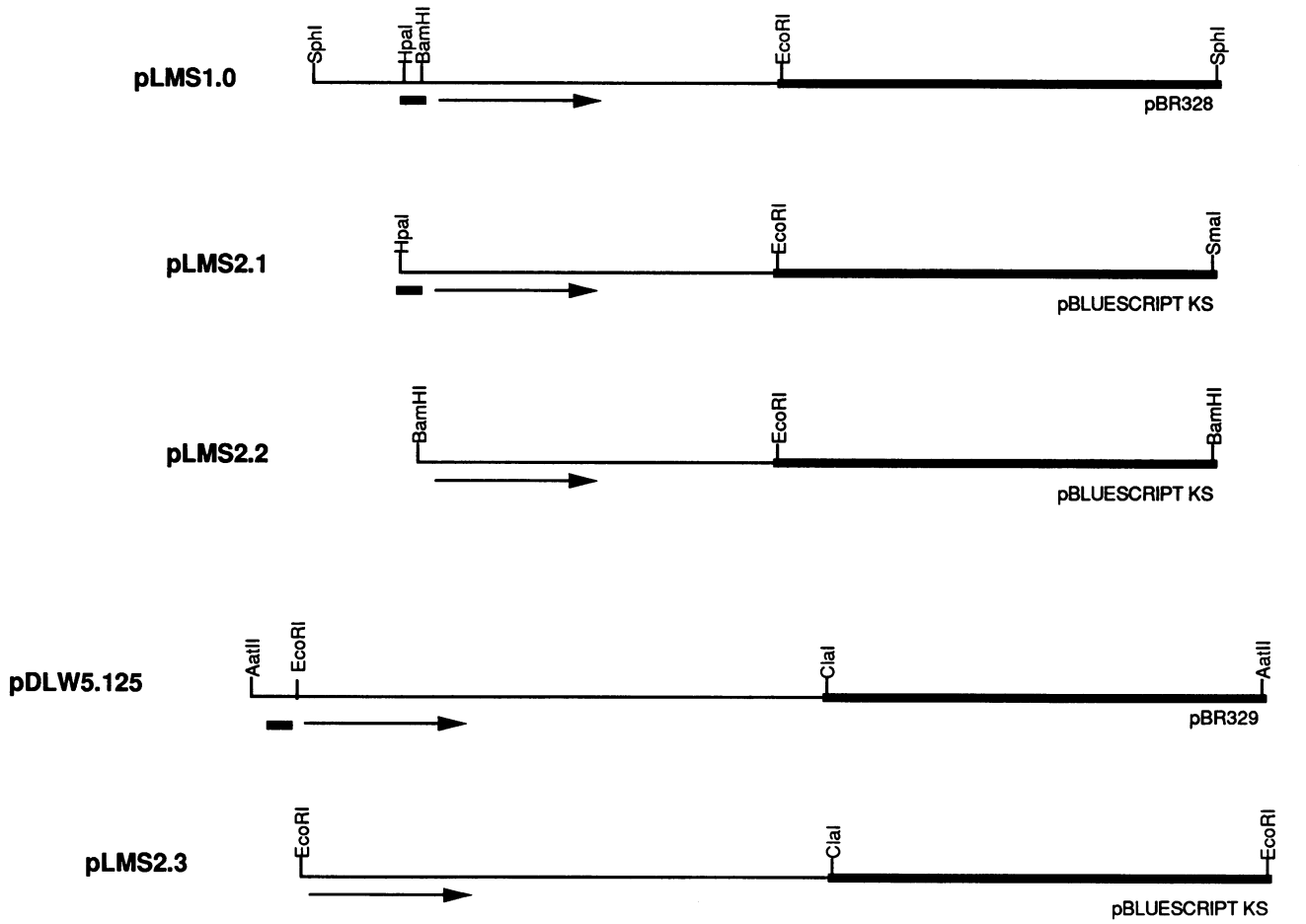

FIG. 6. Shiga-like toxin promoter-deletion subclone strategy. Recombinant plasmids pLMS2.1 and pLMS2.2 are SLT-II operon subclones of pLMS1.0 (Table 1). Recombinant plasmid pLMS2.3 is a SLT-IIv operon subclone of pDLW5.125 (Table 1). Arrows indicate the location of the toxin structural genes and the direction of transcription from the respective promoter (indicated by a solid block upstream of the coding region). Vector DNA is represented by bold lines.

transcriptional efficiency of the *slt*-II/*slt*-IIv promoter was shown to be equivalent to that of the *stx*/*slt*-I promoter under low-iron growth conditions. However, the activity of the *slt*-II/*slt*-IIv promoter, in contrast to that of the *stx*/*slt*-I promoter, was not regulated by the Fur protein and its iron corepressor. The SLT-II operon was demonstrated to be transcribed as a single polycistronic message, and no independent transcript of the *slt*-IIB gene was demonstrated.

TABLE 5. Shiga-like toxin promoter transcriptional efficiencies

Plasmid construct[a]	Promoter	Iron[b]	CAT enzyme (mean ± 2 SEM)[c]
pLMSCATI	*stx*	+	248.5 ± 119.8[d]
		−	1201.9 ± 440.2
pLMSCATII	*slt*-II	+	702.6 ± 97.2
		−	893.4 ± 213.8
pLMSCATC	*lac*	+	3988.9 ± 243.0
		−	3027.8 ± 218.8

[a] As described in Table 1. Four samples tested per group.
[b] +, With added iron; −, without added iron.
[c] CAT enzyme (μg) produced per ml of culture, expressed as mean value ± 2 standard errors of the mean.
[d] Significantly different ($P < 0.05$) by Student's unpaired *t* test from value for the same construct grown in the absence of added iron.

These data indicate that synthesis of the A subunit and B subunit in quantities necessary to account for the single A subunit to multiple B subunit stoichiometry of the SLT-II holotoxin is not a consequence of regulation at the transcriptional level. It is tempting to speculate that the differences in regulation of the type I and type II SLTs by iron could have important consequences for the roles of these toxins in the pathogenesis of infectious diseases caused by SLT-producing *E. coli*. Experimental tests of that hypothesis must await the development of appropriate animal models for diseases such as hemorrhagic colitis and the hemolytic uremic syndrome. Towards this end, a mouse model in which oral infection by SLT-producing *E. coli* causes acute renal tubular necrosis and death was recently developed in our laboratory (45).

ACKNOWLEDGMENT

This work was funded by Public Health Service grant AI 20148-07 from the National Institutes of Health.

LITERATURE CITED

1. **Betley, M. J., V. L. Miller, and J. J. Mekalanos.** 1986. Genetics of bacterial enterotoxins. Annu. Rev. Microbiol. **40**:577–605.
2. **Boyer, H. W., and D. Roulland-Dussoix.** 1969. A complementa-

tion analysis of the restriction and modification of DNA in *Escherichia coli*. J. Mol. Biol. **41**:459–472.
3. **Brendel, V., and E. N. Trifonov.** 1984. A computer algorithm for testing prokaryotic terminators. Nucleic Acids Res. **12**:4411–4427.
4. **Calderwood, S. B., F. Auclair, A. Donohue-Rolfe, G. T. Keusch, and J. J. Mekalanos.** 1987. Nucleotide sequence of the Shiga-like toxin genes of *Escherichia coli*. Proc. Natl. Acad. Sci. USA **84**:4364–4368.
5. **Calderwood, S. B., and J. J. Mekalanos.** 1987. Iron regulation of Shiga-like toxin expression in *Escherichia coli* is mediated by the *fur* locus. J. Bacteriol. **169**:4759–4764.
6. **Chirgwin, J. J., A. E. Przybyla, R. J. MacDonald, and W. J. Rutter.** 1979. Isolation of biologically active ribonucleic acid from sources enriched in ribonuclease. Biochemistry **18**:5294–5299.
7. **De Grandis, S., J. Ginsberg, M. Toone, S. Climie, J. Friesen, and J. Brunton.** 1987. Nucleotide sequence and promoter mapping of the *Escherichia coli* Shiga-like toxin operon of bacteriophage H-19B. J. Bacteriol. **169**:4313–4319.
8. **De Grandis, S., H. Law, J. Brunton, C. Gyles, and C. A. Lingwood.** 1989. Globotetraosylceramide is recognized by the pig edema disease toxin. J. Biol. Chem. **264**:12520–12525.
9. **Donohue-Rolfe, A., G. T. Keusch, C. Edson, D. Thorley-Lawson, and M. Jacewicz.** 1984. Pathogenesis of Shigella diarrhea. IX. Simplified high yield purification of Shigella toxin and characterization of subunit composition and function by the use of subunit specific monoclonal and polyclonal antibodies. J. Exp. Med. **160**:1767–1781.
10. **Dubos, R. J., and J. W. Geiger.** 1946. Preparation and properties of Shiga toxin and toxoid. J. Exp. Med. **84**:143–156.
11. **Endo, Y., K. Mitsui, M. Motizuki, and K. Tsurugi.** 1987. The mechanism of action of ricin and related toxic lectins on eucaryotic ribosomes. The site and the characteristics of the modification in 28S ribosomal RNA caused by the toxins. J. Biol. Chem. **262**:5908–5912.
12. **Endo, Y., K. Tsurugi, T. Yutsudo, Y. Takeda, T. Ogasawara, and K. Igarashi.** 1988. Site of action of a Vero toxin (VT2) from *Escherichia coli* 0157:H7 and of Shiga toxin on eukaryotic ribosomes: RNA N-glycosidase activity of the toxins. Eur. J. Biochem. **171**:45–50.
13. **Federal Register.** 1986. Recombinant DNA research guidelines. Appendix F-IV-H. Fed. Regist. **51**:16972.
14. **Gentry, M., and J. Dalrymple.** 1980. Quantitative microtiter cytotoxicity assay for *Shigella* toxin. J. Clin. Microbiol. **12**:361–366.
15. **Gyles, C. L., S. A. De Grandis, C. MacKenzie, and J. L. Brunton.** 1988. Cloning and nucleotide sequence analysis of the genes determining verocytotoxin production in a porcine edema disease isolate of *Escherichia coli*. Microb. Pathog. **5**:419–426.
16. **Hanahan, D.** 1983. Studies on transformation of *Escherichia coli* with plasmids. J. Mol. Biol. **166**:557–580.
17. **Hantke, K.** 1984. Cloning of the repressor protein gene of iron-regulated systems in *Escherichia coli* K-12. Mol. Gen. Genet. **197**:337–341.
18. **Hawley, D. K., and W. R. McClure.** 1983. Compilation and analysis of *Escherichia coli* promoter DNA sequences. Nucleic Acids Res. **11**:2237–2255.
19. **Jacewicz, M., H. Clausen, E. Nudelman, A. Donohue-Rolfe, and G. T. Keusch.** 1986. Pathogenesis of Shigella diarrhea. XI. Isolation of a Shigella toxin-binding glycolipid from rabbit jejunum and HeLa cells and its identification as globotriaosylceramide. J. Exp. Med. **163**:1391–1404.
20. **Jackson, M. P., R. J. Neill, A. D. O'Brien, R. K. Holmes, and J. W. Newland.** 1987. Nucleotide sequence analysis and comparison of the structural genes for Shiga-like toxin 1 and Shiga-like toxin II encoded by bacteriophages from *Escherichia coli* 933. FEMS Microbiol. Lett. **44**:109–114.
21. **Jackson, M. P., J. W. Newland, R. K. Holmes, and A. D. O'Brien.** 1987. Nucleotide sequence analysis of the structural genes for Shiga-like toxin I encoded by bacteriophage 933J from *Escherichia coli*. Microb. Pathog. **2**:147–153.
22. **Kozlov, Y. U., A. A. Kabishev, E. V. Lukyanov, and A. A. Bayev.** 1988. The primary structure of the operons coding for *Shigella dysenteriae* toxin and temperate phage H30 shiga-like toxin. Gene **67**:213–221.
23. **Lindberg, A. A., J. E. Brown, N. Stromberg, M. Westling-Ryd, J. E. Schultz, and K.-A. Karlsson.** 1987. Identification of the carbohydrate receptor for Shiga toxin produced by *Shigella dysenteriae* type 1. J. Biol. Chem. **262**:1779–1785.
24. **Lindberg, A. A., J. E. Schultz, M. Westling, J. E. Brown, S. W. Rothman, K.-A. Karlsson, and N. Stromberg.** 1986. Identification of the receptor glycolipid for Shiga toxin produced by *Shigella dysenteriae* type 1, p. 439–446. *In* D. Lark (ed.), Protein-carbohydrate interactions in biological systems. Academic Press, Inc. (London), Ltd., London.
25. **Lingwood, C. A., H. Law, S. Richardson, M. Petric, J. L. Brunton, S. D. DeGrandis, and M. Karmali.** 1987. Glycolipid binding of purified and recombinant *Escherichia coli* produced verotoxin *in vitro*. J. Biol. Chem. **262**:8834–8839.
26. **Maniatis, T., E. F. Fritsch, and J. Sambrook.** 1982. Molecular cloning: a laboratory manual. Cold Spring Harbor Laboratory, Cold Spring Harbor, N.Y.
27. **Marques, L. R. M., M. A. Moore, J. G. Wells, I. K. Wachsmuth, and A. D. O'Brien.** 1986. Production of Shiga-like toxin by *Escherichia coli*. J. Infect. Dis. **154**:338–341.
28. **Marques, L. R. M., J. S. M. Peiris, S. J. Cryz, and A. D. O'Brien.** 1987. *Escherichia coli* strains isolated from pigs with edema disease produce a variant of Shiga-like toxin II. FEMS Microbiol. Lett. **44**:33–38.
29. **McIver, J., G. Grady, and G. Keusch.** 1975. Production and characterization of exotoxin(s) of *Shigella dysenteriae* type 1. J. Infect. Dis. **131**:559–566.
30. **Newland, J. W., N. A. Strockbine, S. F. Miller, A. D. O'Brien, and R. K. Holmes.** 1985. Cloning of Shiga-like toxin structural genes from a toxin-converting phage of *Escherichia coli*. Science **230**:179–181.
31. **Newland, J. W., N. A. Strockbine, and R. J. Neill.** 1987. Cloning of genes for production of *Escherichia coli* Shiga-like toxin type II. Infect. Immun. **55**:2675–2680.
32. **O'Brien, A. D., and R. K. Holmes.** 1987. Shiga and Shiga-like toxins. Microbiol. Rev. **51**:206–220.
33. **O'Brien, A. D., J. W. Newland, S. F. Miller, R. K. Holmes, H. W. Smith, and S. B. Formal.** 1984. Shiga-like toxin converting phages from *Escherichia coli* strains that cause hemorrhagic colitis or infantile diarrhea. Science **226**:694–696.
34. **Olsnes, S., R. Reisbig, and K. Eiklid.** 1981. Subunit structure of *Shigella* cytotoxin. J. Biol. Chem. **256**:8732–8738.
35. **Rosenberg, M., and D. Court.** 1979. Regulatory sequences involved in the promotion and termination of RNA transcription. Annu. Rev. Genet. **13**:319–353.
36. **Samuel, J. E., L. P. Perera, S. Ward, A. D. O'Brien, V. Ginsburg, and H. C. Krivan.** 1990. Comparison of the glycolipid receptor specificities of Shiga-like toxin type II and Shiga-like toxin type II variants. Infect. Immun. **58**:611–618.
37. **Sanger, F., S. Nicklen, and A. R. Coulson.** 1977. DNA sequencing with chain-terminating inhibitors. Proc. Natl. Acad. Sci. USA **74**:5463–5467.
38. **Saxena, S. K., A. D. O'Brien, and E. J. Ackerman.** 1989. Shiga toxin, Shiga-like toxin II variant, and ricin are all single-site RNA N-glycosidases of 28S RNA when microinjected into *Xenopus* oocytes. J. Biol. Chem. **264**:596–601.
39. **Selden, R. F.** 1989. Analysis of RNA by Northern hybridization, p. 4.91–4.98. *In* F. M. Ausubel, R. Brent, R. E. Kingston, D. D. Moore, J. G. Seidman, J. A. Smith, and K. Struhl (ed.), Current protocols in molecular biology—1989, vol. 1. Greene Publishing Associates and Wiley Interscience, John Wiley & Sons, Inc., New York.
40. **Smith, W. H., P. Green, and Z. Parsell.** 1983. Vero cell toxins in *Escherichia coli* and related bacteria: transfer by phage and conjugation and toxic action in laboratory animals, chickens, and pigs. J. Gen. Microbiol. **129**:3121–3137.
41. **Strockbine, N. A., M. P. Jackson, L. M. Sung, R. K. Holmes, and A. D. O'Brien.** 1988. Cloning and sequencing of the genes for Shiga toxin from *Shigella dysenteriae* type 1. J. Bacteriol. **170**:1116–1122.

42. **Strockbine, N. A., L. R. M. Marques, J. W. Newland, H. W. Smith, R. K. Holmes, and A. D. O'Brien.** 1986. Two toxin-converting phages from *Escherichia coli* O157:H7 strain 933 encode antigenically distinct toxins with similar biological activities. Infect. Immun. **53**:135–140.
43. **van Heyningen, W. E., and G. P. Gladstone.** 1953. The neurotoxin of *Shigella shigae* 3. The effect of iron on production of toxin. Br. J. Exp. Pathol. **34**:221–229.
44. **Waddell, T., S. Head, M. Petric, A. Cohen, and C. Lingwood.** 1988. Globotriosyl ceramide is specifically recognized by the *Escherichia coli* verocytotoxin. Biochem. Biophys. Res. Commun. **152**:674–679.
45. **Wadolkowski, E. A., J. A. Burris, and A. D. O'Brien.** 1990. Mouse model for colonization and disease caused by enterohemorrhagic *Escherichia coli* O157:H7. Infect. Immun. **58**:2438–2445.
46. **Weinstein, D. L., R. K. Holmes, and A. D. O'Brien.** 1988. Effects of iron and temperature on Shiga-like toxin I production by *Escherichia coli*. Infect. Immun. **56**:106–111.
47. **Weinstein, D. L., M. P. Jackson, L. P. Perera, R. K. Holmes, and A. D. O'Brien.** 1989. In vivo formation of hybrid toxins comprising Shiga toxin and the Shiga-like toxins and role of the B subunit in localization and cytotoxic activity. Infect. Immun. **57**:3743–3750.
48. **Weinstein, D. L., M. P. Jackson, J. E. Samuel, R. K. Holmes, and A. D. O'Brien.** 1988. Cloning and sequencing of a Shiga-like toxin type II variant from an *Escherichia coli* strain responsible for edema disease of swine. J. Bacteriol. **170**:4223–4230.
49. **Yamamoto, T., A. Suyama, N. Mori, T. Yokota, and A. Wada.** 1985. Gene expression in the polycistronic operons of *Escherichia coli* heat-labile toxin and cholera toxin: a new model of translational control. FEBS Lett. **181**:377–380.
50. **Yanisch-Perron, C., J. Vieira, and J. Messing.** 1985. Improved M13 phage cloning vectors and host strains: nucleotide sequences of the M13mp18 and pUC19 vectors. Gene **33**:103–119.